Circulation

ORIGINAL RESEARCH ARTICLE

Lysed Erythrocyte Membranes Promote Vascular Calcification

Possible Role of Erythrocyte-Derived Nitric Oxide

BACKGROUND: Intraplaque hemorrhage promotes atherosclerosis progression, and erythrocytes may contribute to this process. In this study we examined the effects of red blood cells on smooth muscle cell mineralization and vascular calcification and the possible mechanisms involved.

METHODS: Erythrocytes were isolated from human and murine whole blood. Intact and lysed erythrocytes and their membrane fraction or specific erythrocyte components were examined in vitro using diverse calcification assays, ex vivo by using the murine aortic ring calcification model, and in vivo after murine erythrocyte membrane injection into neointimal lesions of hypercholesterolemic apolipoprotein E–deficient mice. Vascular tissues (aortic valves, atherosclerotic carotid artery specimens, abdominal aortic aneurysms) were obtained from patients undergoing surgery.

RESULTS: The membrane fraction of lysed, but not intact human erythrocytes promoted mineralization of human arterial smooth muscle cells in culture, as shown by Alizarin red and van Kossa stain and increased alkaline phosphatase activity, and by increased expression of osteoblast-specific transcription factors (eg, runt-related transcription factor 2, osterix) and differentiation markers (eg, osteopontin, osteocalcin, and osterix). Erythrocyte membranes dose-dependently enhanced calcification in murine aortic rings, and extravasated CD235a-positive erythrocytes or Perl iron-positive signals colocalized with calcified areas or osteoblast-like cells in human vascular lesions. Mechanistically, the osteoinductive activity of lysed erythrocytes was localized to their membrane fraction, did not involve membrane lipids, heme, or iron, and was enhanced after removal of the nitric oxide (NO) scavenger hemoglobin. Lysed erythrocyte membranes enhanced calcification to a similar extent as the NO donor diethylenetriamine-NO, and their osteoinductive effects could be further augmented by arginase-1 inhibition (indirectly increasing NO bioavailability). However, the osteoinductive effects of erythrocyte membranes were reduced in human arterial smooth muscle cells treated with the NO scavenger 2-phenyl-4,4,5,5-tetramethylimidazoline-1-oxyl 3-oxide or following inhibition of NO synthase or the NO receptor soluble guanylate cyclase. Erythrocytes isolated from endothelial NO synthase–deficient mice exhibited a reduced potency to promote calcification in the aortic ring assay and after injection into murine vascular lesions.

CONCLUSIONS: Our findings in cells, genetically modified mice, and human vascular specimens suggest that intraplaque hemorrhage with erythrocyte extravasation and lysis promotes osteoblastic differentiation of smooth muscle cells and vascular lesion calcification, and also support a role for erythrocyte-derived NO.

Dimitrios N. Tziakas, MD
Georgios Chalikias, MD
Maria Pavlaki, PhD
Dimitra Kareli, PhD
Rajinikanth Gogiraju, PhD
Astrid Hubert, PhD
Elsa Böhm
Petros Stamoulis, MSc
Ioannis Drosos, MD
Petros Kikas, MD
Dimitrios Mikroulis, MD
Alexandra Giatromanolaki, MD
George S. Georgiadis, MD
Fotios Konstantinou, MD
Christos Argyriou, MD
Thomas Münzel, MD
Stavros V. Konstantinides, MD
Katrin Schäfer, MD

Key Words: atherosclerosis ■ erythrocytes ■ hemorrhage ■ smooth muscle, myocytes ■ vascular calcification

Sources of Funding, see page 2046

https://www.ahajournals.org/journal/circ

Clinical Perspective

What Is New?

- Lysed erythrocytes, and in particular their membrane fraction, enhanced human and murine arterial smooth muscle cell mineralization, and vascular (aortic ring) calcification.
- Red blood cell membrane injection into vascular lesions of atherosclerosis-prone mice also promoted calcification, and red blood cells were found to colocalize with osteoblast-like cells in human atherosclerotic plaques, stenotic aortic valves, and abdominal aortic aneurysms.
- Genetic deletion or pharmacological blockade of endothelial nitric oxide (NO) synthase, or inhibition of the NO receptor soluble guanylate cyclase in smooth muscle cells, reduced the osteoinductive effects of red blood cell membranes, and erythrocytes isolated from endothelial NO synthase–deficient mice were less potent in inducing calcification.

What Are the Clinical Implications?

- Intraplaque hemorrhage promotes atherosclerotic and valvular lesion calcification.
- Membranes of extravasated, lysed red blood cells appear to play an important role in this process, and NO derived from erythrocyte endothelial NO synthase is involved, at least in part, in mediating the effects of red blood cells on vascular calcification.
- Conditions influencing red blood cell stability and their susceptibility to lysis under mechanical, osmotic, or other local stress, and factors selectively targeting red blood cell NO release, as well, may represent potential therapeutic targets to reduce calcific valvular disease and, possibly, atherosclerosis progression.

The deposition of calcium hydroxyapatite minerals is a typical feature of advanced atherosclerotic and valvular lesions. Ectopic vascular calcification occurs primarily at the aorta, aortic valve, and coronary arteries.[1] Microcalcifications, in particular those embedded in the fibrous cap, have been found to promote plaque instability and rupture by increasing local tissue stress,[2] thus adding to the effects of neovascularization, inflammation, matrix metalloproteinase expression, and smooth muscle cell death.

Vascular calcification is an actively regulated process, very similar to embryonic skeletal bone formation. Cells of the vessel wall assume an osteoblast-like phenotype and upregulate specific transcription factors, resulting in the expression of extracellular matrix proteins and the incorporation of hydroxyapatite crystals.[3] Osteoblast and bone markers have been detected in calcified human aortic valves and arteries,[4,5] and in aged apolipoprotein E–deficient mice.[6] Factors promoting vascular calcification include age, hypertension, diabetes mellitus, end-stage renal disease, and smoking.

Although the presence of extravasated erythrocytes in human atherosclerotic lesions was described several years ago,[7] little is known about a possible active role of red blood cells (RBCs) during cardiovascular disease processes. Clinical studies suggested that intraplaque hemorrhage may be associated with the progression of coronary[8] and carotid[9] atherosclerotic lesions and degenerative calcific aortic valve stenosis.[10] Our own group previously reported that the total cholesterol content in the membrane of circulating erythrocytes was associated with the clinical presentation of coronary artery disease and was significantly elevated in patients with acute coronary syndromes.[11,12] Moreover, we could show in rabbits fed an atherogenic diet that statin treatment correlated with reduced erythrocyte cholesterol levels, and significantly smaller lipid cores, fewer macrophages, and fewer microvessels, as well.[13] Further evidence indirectly supporting a causal role of erythrocytes came from studies showing that atherosclerotic lesion progression in apolipoprotein E knockout mice was significantly reduced after the induction of anemia by using phenylhydrazine.[14]

In the present study, we examined the contribution of erythrocytes to vascular and valvular lesion progression, focusing on the effects of RBCs on the osteoblastic transdifferentiation of smooth muscle cells and calcification. We also dissected the possible mechanisms underlying the osteoinductive effects of lysed erythrocyte membranes.

METHODS

The data and methods that support the findings of this study are available from the corresponding author on reasonable request. A detailed description of the materials and methods is provided in the online-only Data Supplement Material.

Isolation of Erythrocytes and Erythrocyte Membranes

Erythrocytes were isolated using density gradient centrifugation, as described.[11,15] In brief, anticoagulated whole blood was centrifuged at 1500*g* for 10 minutes. Plasma, platelets, and buffy coat were removed, and the pellet containing RBCs was washed with 1× PBS followed by additional purification over Histopaque-1119 (Sigma). The purity of the RBC preparation was examined using flow cytometry (Figure I in the online-only Data Supplement). Intact erythrocytes were immediately lysed in ice-cold hypotonic lysis buffer and either stored at –80°C pending analysis, or erythrocyte membranes were prepared from an aliquot by repeated centrifugation and washing in PBS (representative examples are shown in Figure IIA in the online-only Data Supplement). Contamination with hemoglobin or heme was excluded using the Hemoglobin or Heme Assay kit (Sigma), respectively (Figure IIB through IID in the online-only Data Supplement). Lipids (cholesterol, phospholipids) were extracted from human erythrocyte

membranes following a published protocol[16] and quantified using the Cholesterol Quantitation Kit (BioAssay Systems). Heme was isolated from whole blood as described.[17]

Smooth Muscle Cell Cultivation and Osteoblastic Differentiation

Human arterial smooth muscle cells (HASMCs; PromoCell) and murine arterial smooth muscle cells (American Type Culture Collection ATCC) were cultivated in DMEM (GlutaMAX-I) containing $CaCl_2$ (4 mmol/L; Sigma), β-glycerophosphate (5 mmol/L; Sigma), L-ascorbic acid (50 μg/mL; Sigma), insulin (1 μmol/L; Sigma), and dexamethasone (0.1 μmol/L; Sigma) (osteogenic medium). To visualize calcium deposition, HASMCs were fixed and incubated with 0.4 mg/mL Alizarin red S solution (pH 4.2). The dye was extracted using 10% acetic acid followed by colorimetric detection at 405 nm.[18] Phosphate deposits were visualized using 5% silver nitrate and UV light (van Kossa stain). To determine alkaline phosphatase activity, cells were incubated with 5-bromo-4-chloro-3-indolyl phosphate/nitro blue tetrazolium substrate solution (Sigma). NO release was determined by measuring nitrite/nitrate using Griess Reagent System (Promega).

Aortic Ring Calcification Assay

Descending aortas were prepared from 8- to 10-week-old C57BL6 mice (wild-type; Janvier Labs) or endothelial NO synthase (eNOS)–deficient mice ($eNOS^{-/-}$; Jackson Laboratories), cut into 2- to 3-mm rings, and placed into DMEM or osteogenic medium together with erythrocyte membranes isolated from wild-type or $eNOS^{-/-}$ mice. Rings were paraffin-embedded, and transverse sections were stained using Alizarin red.

Murine Atherosclerosis

Vascular injury and neointima formation were induced in male apolipoprotein E–deficient mice ($apoE^{-/-}$; Jackson Laboratories) fed Western-type diet (TD 88137; Harlan Teklad). On day 21 after injury, erythrocyte membranes from wild-type or $eNOS^{-/-}$ mice were injected into the neointima. Vascular calcification was examined 1, 2, and 6 weeks later. Plasma cholesterol levels were determined by using the EnzyChrom HDL and LDL/VLDL Assay kit (BioAssay Systems). All animal experiments had been approved by the institutional Animal Research Committee and the state authorities and complied with institutional and national guidelines for the care and use of laboratory animals.

Human Vascular Specimens

Calcified stenotic aortic valves, abdominal aortic aneurysm specimens, and atherosclerotic carotid artery plaques were obtained from symptomatic patients undergoing elective surgery at the University General Hospital of Alexandroupolis, Greece, Departments of Cardiothoracic Surgery and Vascular Surgery, respectively. Patients with active cancer or with systemic inflammatory or autoimmune disease were excluded. Tissue specimens were immediately processed for either paraffin or cryo embedding. The study protocol complied with the declaration of Helsinki and was approved by the institutional review board. All participants were informed and gave their signed consent before inclusion in the study.

Histological and Immunohistochemical Analyses

Paraffin-embedded human and mouse vascular tissues were stained using Masson Goldner trichrome to detect erythrocytes (bright red), connective tissue (light green), and bone structures (green). Calcification (red signal) was assessed using Alizarin red and van Kossa staining or 5-bromo-4-chloro-3-indolyl phosphate/nitro blue tetrazolium as a substrate for alkaline phosphatase. Perl iron stain was used to detect tissue iron. Immunohistochemical analysis was performed using antibodies against eNOS (Novus Biologicals), glycophorin A (CD235a; Dako), hemoglobin (Abcam), methemoglobin (LifeSpan Biosciences), osteopontin (Abcam), osterix (Abcam), smooth muscle actin (Sigma), or TER-119 (R&D Systems) and examined under an Olympus BX51 microscope using image analysis software (Image-Pro Plus; Media Cybernetics). Immunofluorescence and confocal microscopy analyses were performed on cryo-embedded tissue sections using primary antibodies against CD235a, osteopontin, or eNOS (Santa Cruz Biotechnology) followed by fluorescence-labeled donkey anti-mouse or donkey anti-rabbit secondary antibodies (Life Technologies) and Hoechst solution (Thermo Scientific). Sections were examined under an Andor Revolution XD spinning disc confocal Olympus IX81 microscope. Images were analyzed using ImageJ 1.50i software.

Western Blot and Immunoprecipitation

eNOS was immunoprecipitated from erythrocyte lysates using a rabbit polyclonal antibody against eNOS (Santa Cruz Biotechnology) and protein G agarose beads (Millipore). Immunoprecipitated eNOS, and human umbilical vein endothelial cell lysate (positive control), as well, were separated by SDS-PAGE, electroblotted on nitrocellulose membranes, and immunoblotted for eNOS by using the same antibody used for immunoprecipitation. The flow-through was immunoblotted for arginase-1 using a rabbit polyclonal antibody (GeneTex). Mouse monoclonal antibodies against GAPDH (HyTest) were used for normalization. Relative quantification of bands was performed using Image Laboratory 5.0 software (BioRad) and expressed as fold change in comparison with band densities of the same control sample (set at 1) run in all experiments as reference allowing for valid comparisons in band density quantification.

RNA Isolation and Quantitative Real-Time Polymerase Chain Reaction Analysis

Cells were homogenized in TRI Reagent (Ambion). Total RNA was isolated and the amount and quality checked by spectrophotometry (μCuvette G1.0; Eppendorf). One microgram of RNA was reversed-transcribed into cDNA by using M-MLV Reverse Transcriptase (Promega) followed by quantitative real-time polymerase chain reaction. The primer sequences and conditions are listed in Table I in the online-only Data Supplement.

Statistical Analysis

Data are presented as mean±SEM. Normal distribution was examined using the D'Agostino and Pearson omnibus

normality test. Differences between 2 groups were tested by the Student *t* test for unpaired means. If >2 groups were compared, the 1-way ANOVA test was performed, followed by the Sidak multiple comparison test. Nonparametric tests (Mann-Whitney or Kruskal-Wallis test followed by Dunn multiple comparisons test) were used if samples were not normally distributed. A *P* value <0.05 was considered statistically significant. Analyses were performed using GraphPad PRISM data analysis software (version 6.03; GraphPad Software Inc).

RESULTS

Lysed Erythrocyte Membranes Promote Smooth Muscle Cell Calcification Under Osteogenic Conditions

To examine the effect of RBCs on vascular calcification, HASMCs were cultivated under osteogenic conditions, alone or in the presence of intact or lysed human erythrocytes. Taking into account the physiological RBC count in human whole blood and the technical limitations of the assay, cells were exposed to 1.5×10^6 to 1.5×10^8 erythrocytes for 7 days (with medium change on day 4). As shown in Figure IIIA in the online-only Data Supplement, 1.5×10^8 lysed (corresponding to the number present in 30–40 μL whole blood), but not the same number of intact erythrocytes, markedly enhanced calcium deposition (red signal) as demonstrated by Alizarin red staining. Smaller calcium deposits were detected microscopically in cells exposed to 1.5×10^7, but not in those incubated with 1.5×10^6 lysed erythrocytes (Figure IIIB in the online-only Data Supplement). We could exclude that contamination with plasma or the presence of iron might have contributed to the observed osteogenic effects of lysed erythrocytes (not shown).

Osteogenic Mediators Are Predominantly Located in the Erythrocyte Membrane Fraction

To determine the localization of the osteoinductive component(s) within the cellular compartments of RBCs, the osteogenic effects of total erythrocyte lysates (consisting of cytoplasm and membranes) were compared with those of purified erythrocyte membranes alone. In preliminary experiments, we had determined that erythrocyte membranes account for ≈1% of the total erythrocyte protein content. Because lysed RBCs or their membranes cannot be counted, the amount of erythrocyte membranes was adjusted to represent 1% of the total protein present in 1.5×10^8 erythrocytes, ie, the amount inducing osteoblastic differentiation of HASMCs. As shown in Figure 1A (macroscopic view) and Figure 1B (microscopic images), exposure of HASMCs to erythrocyte membranes, but not the same amount of protein obtained from whole blood, intact or lysed erythrocytes, induced calcium deposition. The results of the quantitative analysis in 10 independent experiments with erythrocytes prepared from 10 different donors are shown in Figure 1C.

Lysed erythrocyte membranes promoted calcium deposition in HASMCs only in the presence of osteogenic medium, but not in cells cultivated in DMEM (Figure IIIC and IIID in the online-only Data Supplement). Neither cholesterol nor the lipid fraction of erythrocyte membranes exhibited osteogenic effects (Figure IIIC and IIID in the online-only Data Supplement). In addition to Alizarin red staining (Figure 1D), the dose-dependent osteoinductive effect of lysed erythrocyte membranes on HASMCs was confirmed by the detection of phosphate deposits (van Kossa stain; black-brown signal; Figure 1E) and alkaline phosphatase activity (5-bromo-4-chloro-3-indolyl phosphate/nitro blue tetrazolium substrate conversion; black-blue signal; Figure 1F). The effects were similar if membranes were isolated from erythrocytes lysed 10, 20, 45, or 60 minutes (Figure IIIE and IIIF in the online-only Data Supplement). Mouse erythrocyte membranes also dose-dependently enhanced the calcification of murine aortic rings ex vivo (Figure 2A and 2B).

Osteogenic Effects of Lysed Erythrocyte Membranes Require Removal of Hemoglobin

Hemoglobin is a major component of erythrocytes, accounting for >90% of their protein content. As explained in Methods, only minimal amounts of heme and hemoglobin were left in erythrocyte membrane preparations at the end of the isolation procedure. To examine the importance of hemoglobin as an osteogenic mediator, we then normalized the amount of lysed erythrocytes or their membranes added to the HASMCs to either the same amount of total protein (Figure IVA and IVB in the online-only Data Supplement) or of hemoglobin detected in erythrocyte membrane preparations (Figure IVC and IVD in the online-only Data Supplement). This procedure revealed that the exposure of HASMCs to erythrocyte membranes is sufficient to induce calcium deposition, and that calcification is not mediated by residual heme or hemoglobin contamination. In fact, adding heme isolated from lysed erythrocytes back to erythrocyte membranes abolished their osteogenic effects and reduced them to those observed in lysed erythrocytes (Figure IVE and IVF in the online-only Data Supplement).

Erythrocytes Colocalize With Vascular Calcification Sites in Human Atherosclerotic Lesions

Sections through diverse human vascular lesions, such as carotid artery atherosclerotic plaque (n=5), aortic

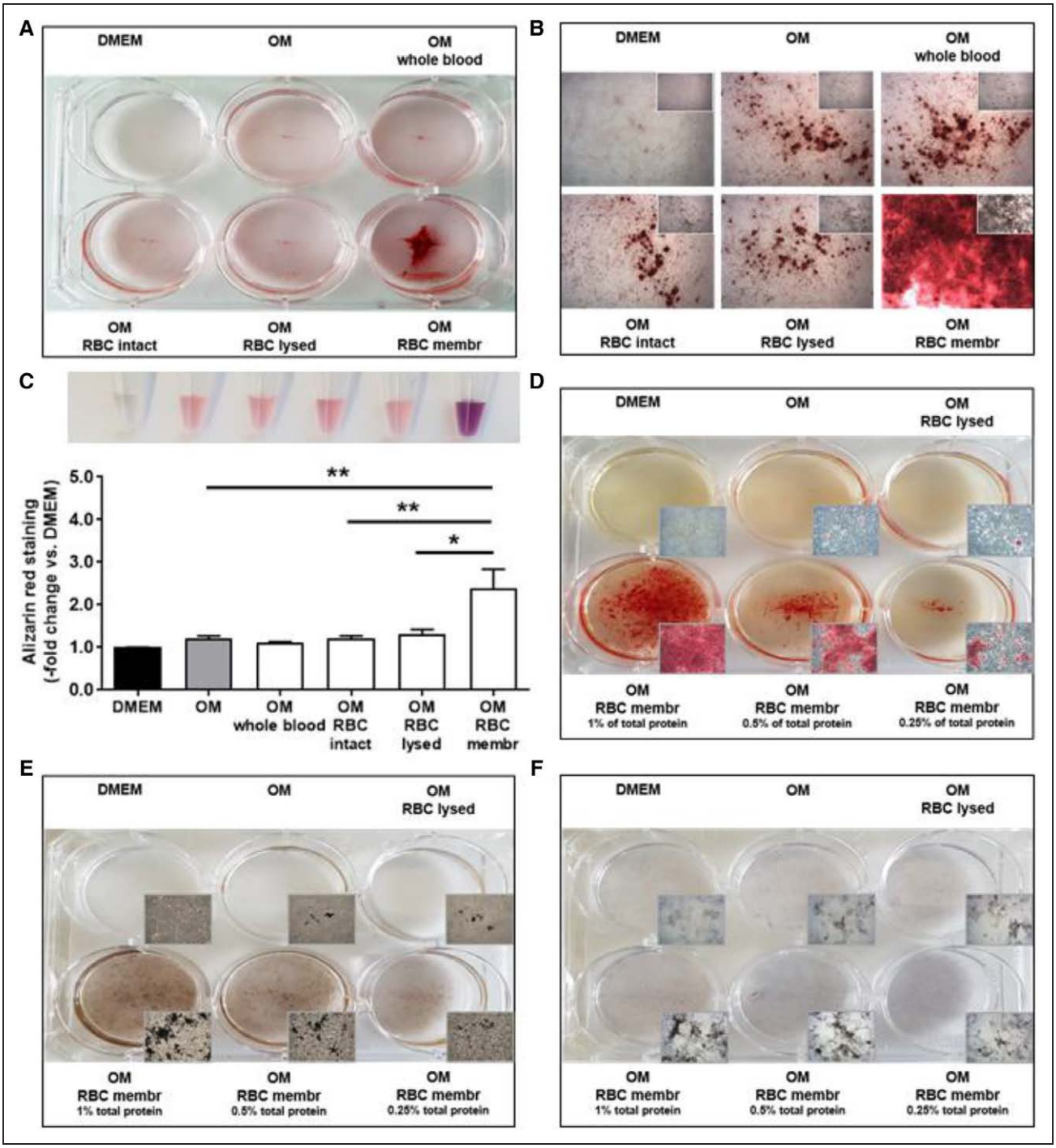

Figure 1. Effect of erythrocytes on human smooth muscle cell calcification in vitro.
HASMCs were seeded in 6-well plates, grown to subconfluence and cultivated for 7 days in DMEM or, osteogenic medium (OM) with or without the addition of equal amounts of intact or lysed red blood cells (RBC) or RBC membrane (membr) protein. Calcium deposition was visualized using Alizarin red stain (red signal). Representative macroscopic (**A**, **D** through **F**) and microscopic (**B**; insets in **D** through **F**) findings are shown. Insets in **B** show unstained cells at day 7. The summary of findings in 10 biological replicates is given in **C**. Samples after Alizarin red extraction are also shown. **P*<0.05 and ***P*<0.01. Dose-dependent effects of RBC membranes: calcium deposits are stained using Alizarin red (**D**), phosphate using van Kossa stain (**E**), and alkaline phosphatase activity using BCIP/NBT as substrate (**F**). Results shown in **C** were analyzed using 1-way ANOVA followed by Sidak multiple comparisons test. BCIP indicates 5-bromo-4-chloro-3-indolyl phosphate; HASMC, human arterial smooth muscle cell; and NBT, nitro blue tetrazolium.

aneurysm (n=8), and stenotic aortic valve tissue specimens (n=13), were stained with Masson Goldner trichrome or antibodies against the erythrocyte membrane protein glycophorin A (CD235a) to detect RBCs, and with antibodies against osteopontin, as well, to detect osteoblasts or Alizarin red to visualize calcification. Confirming earlier histological findings of intralesional hemorrhage, extravasated erythrocytes

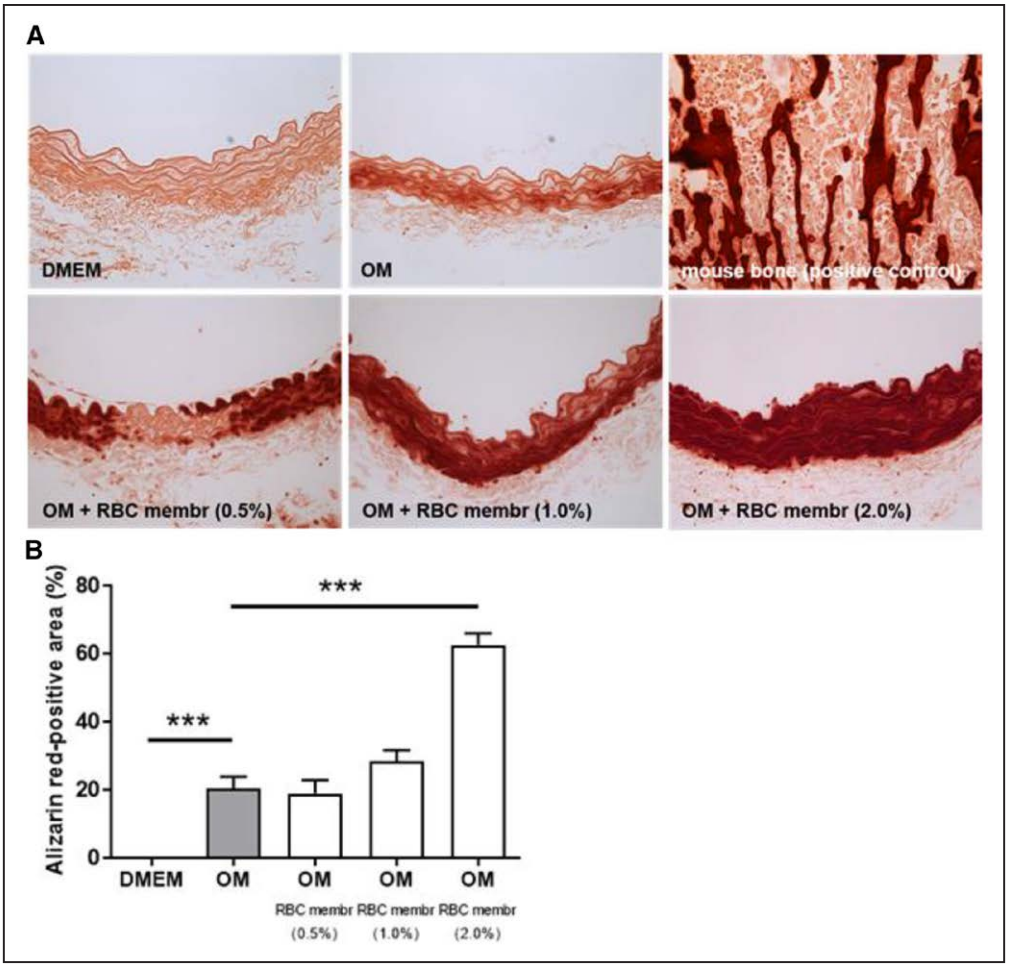

Figure 2. Effect of erythrocyte membranes on murine smooth muscle cell calcification ex vivo.
Murine aortic rings were incubated in DMEM or, osteogenic medium (OM), with or without RBC membranes (membr; 0.5%, 1.0%, or 2.0% of total RBC membrane protein) for 7 days. Aortic rings were embedded in paraffin and 5-µm-thick cross-sections stained with Alizarin red (red signal). Mouse bone was used as positive control. Representative findings (**A**; ×400 magnification) and the results of the quantitative analysis of 3 to 5 aortic rings per variable (**B**) are shown. ***P<0.001. Results shown in **B** were analyzed using 1-way ANOVA followed by Sidak multiple comparisons test. RBC indicates red blood cells.

were detected in 86% of the examined vascular tissue specimens. Analysis of serial sections suggested a close neighborhood of intraplaque erythrocytes with osteopontin-positive osteoblasts (in atherosclerotic plaques, aneurysms) or Alizarin red–positive calcified areas (in calcific aortic valves). Representative images are shown in Figure 3A. Similar results were obtained after Perl iron stain to visualize iron (released from lysed erythrocytes) and using antibodies against osterix (Figure 3B). Fluorescence microscopic analysis of cryosections simultaneously incubated with antibodies against CD235a and osteopontin followed by confocal microscopy provided further support for the colocalization of erythrocyte membranes with osteoblastic cells within vascular lesions (Figure 3C). Quantitative analysis revealed that 86% of all areas with calcification were CD235a-positive, 72% were hemoglobin-positive, and 56% were positive for both (representative findings in Figure VA in the online-only Data Supplement). The extent of the CD235a immunosignal was not associated with the patients' age (r^2=0.007; P=0.753). However, 90% of all areas without calcification contained only hemoglobin (Figure VB in the online-only Data Supplement). Of note, the majority of hemoglobin within vascular lesions was found to be in the form of methemoglobin, in which iron heme is oxidized to the ferric ($^{3+}$) form. Representative examples are shown in Figure VC in the online-only Data Supplement.

Osteogenic Effects of Erythrocyte Membranes Involve NO

Erythrocytes have been shown to express eNOS localized at the cytoplasmic side of the RBC membrane.[19,20] In the present study, confocal microscopy analysis confirmed the presence of eNOS in erythrocytes within human aortic valve specimens (Figure 4A). Immunoprecipitation analysis demonstrated eNOS protein expression in human RBC lysates from healthy individuals and patients with coronary artery disease (Figure 4B through 4D).

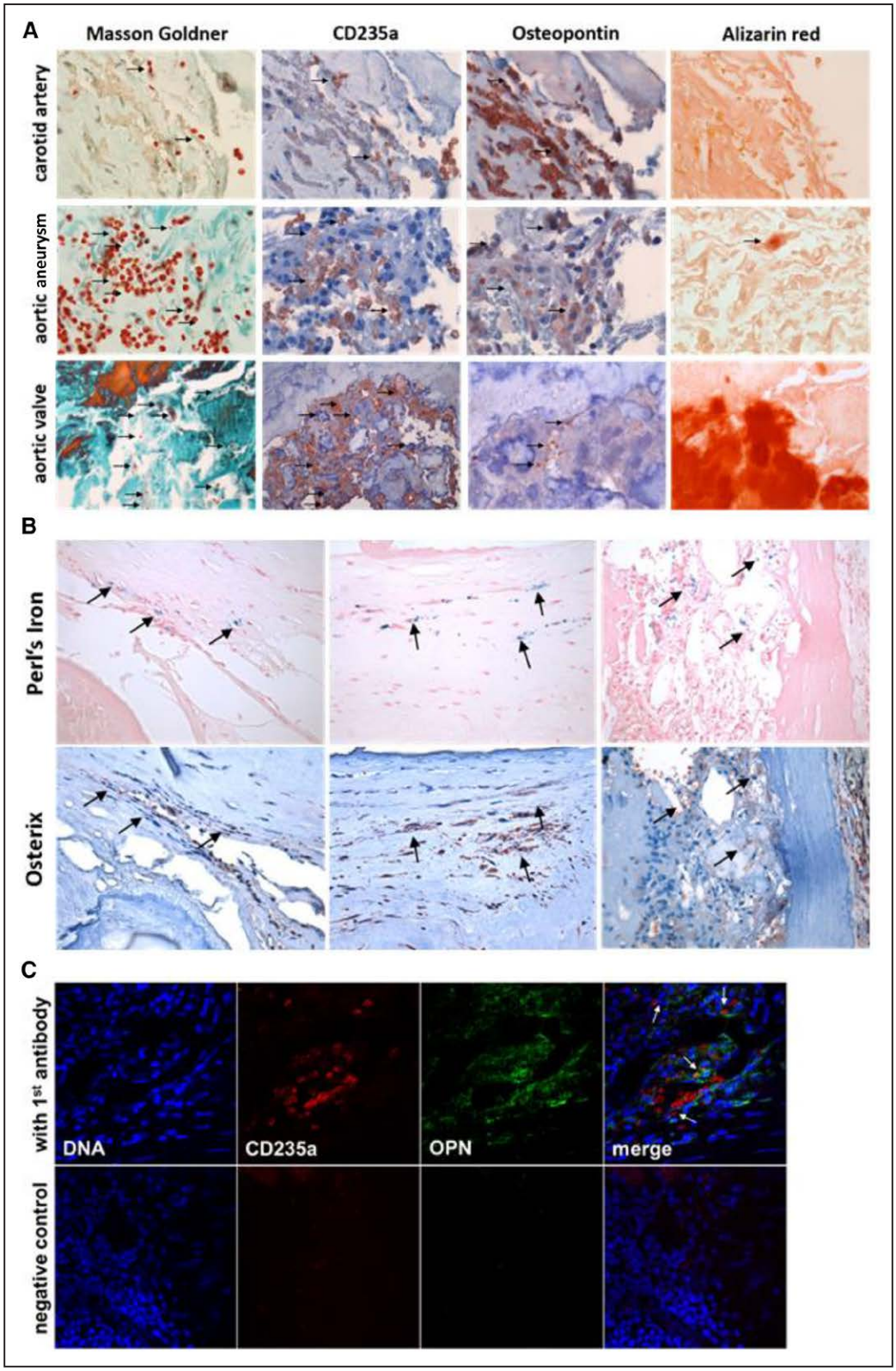

Figure 3. Presence of erythrocytes and calcification in human vascular specimens.
A, Serial cross-sections through human carotid artery atherosclerotic plaques (n=5), aortic aneurysms (n=8), and stenotic aortic valves (n=13) were stained with Masson Goldner trichrome to detect red blood cells (red) and connective tissue (green), Alizarin red to detect calcium deposits (red) or with antibodies against the erythrocyte membrane protein glycophorin A (CD235a; red-brown), or the osteoblast marker osteopontin (OPN; red-brown). ×400 magnification. Arrows point to erythrocytes colocalizing with markers of osteoblastogenesis or calcification on neighboring sections. **B**, Serial cross-sections were stained with Perl iron (blue) or with antibodies against osterix (red-brown). ×200 magnification. Arrows point to iron deposits colocalizing with osteoblasts on neighboring sections. **C**, Cryo-sections through aortic valves were coincubated with antibodies against CD235a and OPN and examined using confocal microscopy. ×400 magnification. White arrows point to double-positive cells.

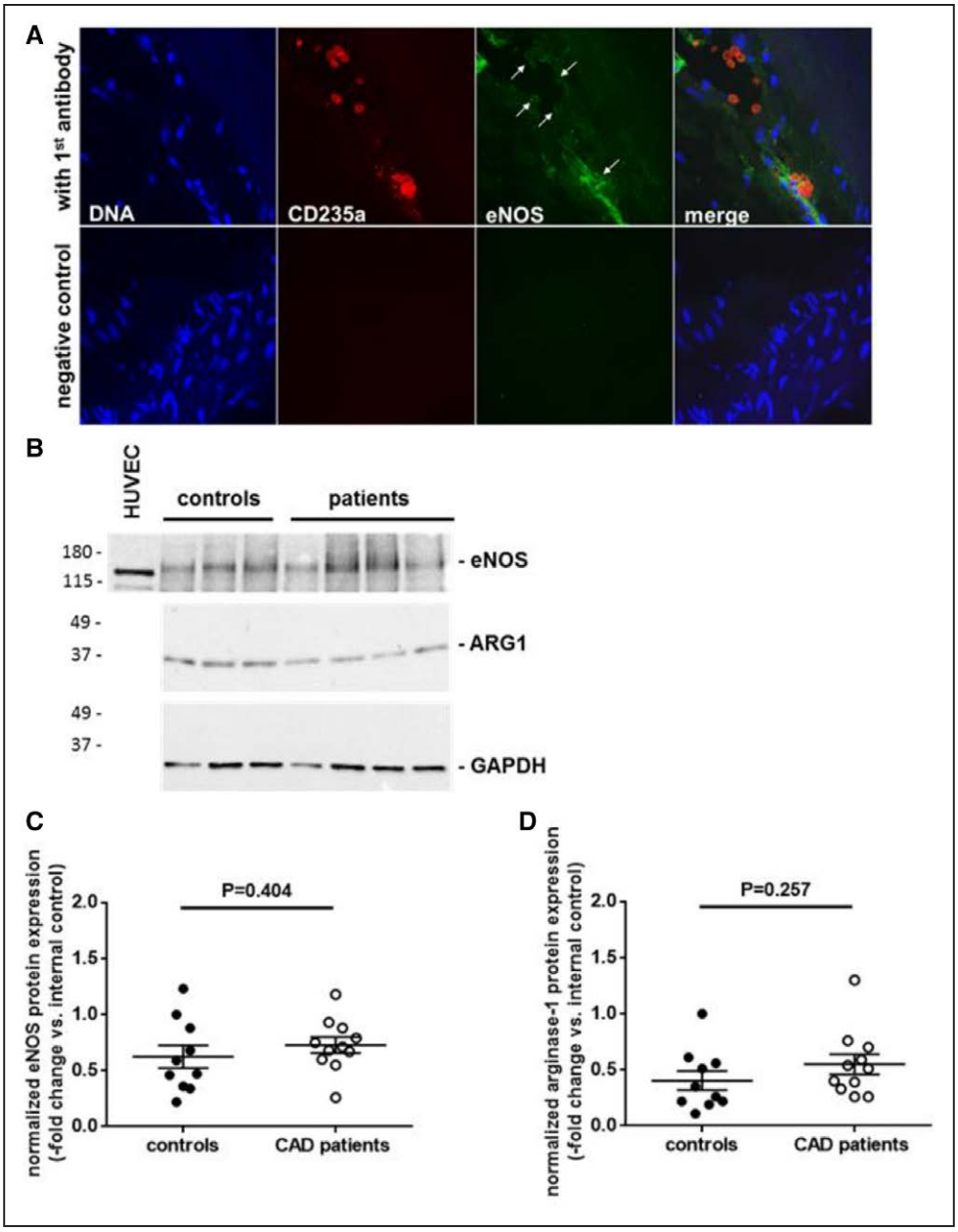

Figure 4. Importance of human erythrocyte eNOS.
A, Cryo-sections through aortic valves were coincubated with antibodies against CD235a and eNOS followed by fluorescence-labeled secondary antibodies and confocal microscopy. ×400 magnification. Representative findings are shown. **B** through **D**, Erythrocytes were isolated from 10 healthy controls and 11 patients with coronary artery disease. Total protein was isolated from RBC lysates and examined for the expression of eNOS using immunoprecipitation (**B** and **C**) and arginase-1 (ARG1) using Western blot (**B** and **D**). GAPDH was used as loading control. Representative membranes of 3 controls and 4 patients are shown (**B**). The relative quantification of eNOS (**C**) and ARG1 (**D**) using GAPDH for normalization is shown. The *y* axis displays the -fold change versus a control sample used as reference (set at 1). Results shown in **C** were normally distributed and analyzed using the Student *t* test for unpaired means. Results shown in **D** were not normally distributed (patients with CAD) and analyzed using the Mann-Whitney test for unpaired means. CAD indicates coronary artery disease; eNOS, endothelial nitric oxide synthase; HUVEC, human umbilical vein endothelial cell; and RBC, red blood cell.

To examine the possibility that the osteogenic effects of erythrocyte membranes involve NO, a series of experiments was performed. Use of the Alizarin red in vitro assay, coincubation of HASMCs with 2-phenyl-4,4,5,5-tetramethylimidazoline-1-oxyl 3-oxide, a stable radical scavenger for NO, significantly reduced the osteogenic activity of erythrocyte membranes (Figure 5A and 5C), whereas the addition of L-norvaline, an inhibitor of arginase-1 increasing NO bioavailability, significantly enhanced calcium deposition (Figure 5A through 5C). Similar findings were observed after incubation of HASMCs alone under osteogenic conditions with the NO donor diethylenetriamine-NO (Figure VIA and VIB in the online-only Data Supplement). Of note, the effects of L-norvaline could be abolished by simultaneous incubation with 2-phenyl-4,4,5,5-tetramethylimidazoline-

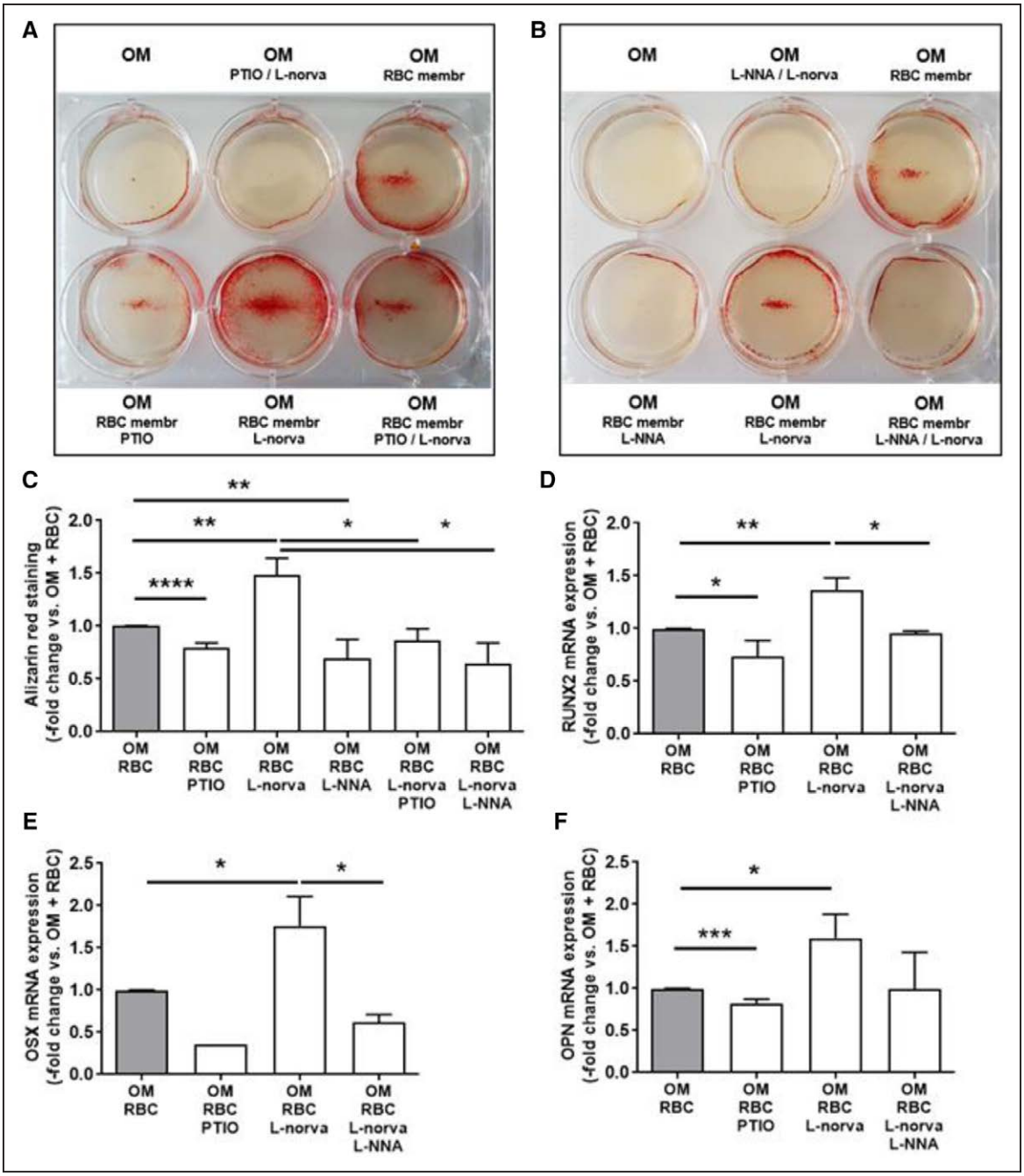

Figure 5. Effect of NO and eNOS modulation on smooth muscle cell calcification.
HASMCs were cultivated for 7 days in osteogenic medium (OM) with or without the addition of red blood cell (RBC) membranes (membr), and PTIO (100 μmol/L) (**A**) or L-NNA (5 μmol/L) (**B**), as well, and L-norvaline (50 nmol/L). Calcium was visualized using Alizarin red (red signal). Representative macroscopic findings are shown in **A** and **B**; the results after quantitative analysis of 5 independent experiments are shown in **C**. Total RNA was isolated from HASMCs and the mRNA expression of RUNX2 (**D**), osterix (OSX; **E**), and osteopontin (OPN; **F**) examined using qPCR. Findings in 5 independent experiments are shown. **P*<0.05, ***P*<0.01, ****P*<0.001, and *****P*<0.0001. Results shown in **C** to **F** were analyzed using 1-way ANOVA followed by Sidak multiple comparisons test. eNOS indicates endothelial nitric oxide synthase; HASMC, human arterial smooth muscle cell; L-NNA, NG-nitro-L-arginine; NO, nitric oxide; L-norva, L-norvaline; PTIO, 2-phenyl-4,4,5,5-tetramethylimidazoline-1-oxyl 3-oxide; qPCR, quantitative polymerase chain reaction; and RUNX2, runt-related transcription factor-2.

1-oxyl 3-oxide (Figure 5A and 5C) or the NO synthase (NOS) inhibitor NG-nitro-L-arginine (Figure 5B and 5C), further supporting the role of eNOS-NO in the osteogenic effects of lysed erythrocytes membranes.

The effects of modulation of NO on osteoblastogenesis were confirmed by using quantitative polymerase chain reaction analysis of runt-related transcription factor-2 (RUNX2) (Figure 5D), osterix (Figure 5E), and osteopontin (Figure 5F). Significantly higher amounts of NO (or its stable metabolite nitrite) were detected in conditioned medium of HASMCs incubated with erythrocyte membranes and decreased in the presence of NG-nitro-L-arginine (Figure VIC in the online-only Data Supplement). Of note, the amount of NO (or its stable

metabolite nitrite) measured in lysed erythrocytes was not affected by lysis duration (Figure VID in the online-only Data Supplement). The osteoinductive effects of RBC membranes could not be reversed by radical scavengers (ie, superoxide dismutase and catalase; Figure VIE and VIF in the online-only Data Supplement).

Short pretreatment of RBC membranes with moderate heat (50°C) increased NO release ($P<0.01$; not shown), similar to a previous report in endothelial cells,[21] and markedly enhanced HASMC calcification, in part in a NO-dependent manner (Figure VIIA and VIIB in the online-only Data Supplement). Conversely, inhibition of eNOS activity in RBC membranes by thiol residue alkylation using *N*-ethylmaleimide[22] dose-dependently reduced their osteogenic activities (Figure VIIC and VIID in the online-only Data Supplement).

Lysed Erythrocyte Membranes Induce Osteogenic Differentiation of Human Smooth Muscle Cells via NO Signaling

To further examine the mechanisms underlying the osteoinductive effects of lysed erythrocyte membranes, HASMCs were coincubated with erythrocyte membranes for 7 days, and osteoblastic differentiation was examined by using quantitative real-time reverse transcription polymerase chain reaction. As shown in Figure 6A, increased expression of RUNX2, a central regulator of osteoblast differentiation,[23] was detected in HASMCs incubated with erythrocyte membranes in comparison with osteogenic medium alone. Also, increased mRNA levels of the transcription factor osterix (Figure 6B) and the osteoblast markers and RUNX2 target genes osteopontin (Figure 6C), bone morphogenetic protein-2 (Figure 6D), and osteocalcin (Figure 6E) were observed after the 7-day incubation of HASMCs with erythrocyte membranes under osteogenic conditions. Of note, unchanged BAX (Bcl-2-associated X protein; Figure VIIIA in the online-only Data Supplement) and increased BCL2 (B-cell lymphoma 2; Figure VIIIB in the online-only Data Supplement) mRNA levels suggested that the observed increased vascular calcification had not occurred secondary to increased apoptotic cell death. Inhibition of the intracellular NO receptor soluble guanylate cyclase (sGC) using 1*H*-[1,2,4]oxadiazolo-[4,3-*a*]quinoxalin-1-one significantly reduced the erythrocyte membrane–induced increase of osteoblast marker mRNA expression (Figure 6A through 6E), and RUNX2 protein levels (Figure 6F and 6G) and calcium deposition (Figure 6H and 6I) in HASMCs, as well.

Osteogenic Effects of Erythrocyte Membranes Ex Vivo Depend on Erythrocyte eNOS

Murine aortic rings isolated from either wild-type or eNOS-deficient mice were coincubated with erythrocyte membranes isolated from either wild-type or eNOS-deficient mice. These studies confirmed the importance of erythrocyte-derived eNOS (as opposed to eNOS present in the vessel wall) for the osteogenic potential of RBCs. Representative findings are shown in Figure 7A; the summary of the quantitative analysis of at least 4 independent experiments is shown in Figure 7B. It is important to note that erythrocytes isolated from eNOS-deficient mice also exhibited a reduced potential to induce the expression of osteoblastic markers, such as RUNX2 (Figure 7C) or the osteoblast-specific transcription factor osterix (Figure 7D) in murine aortic smooth muscle cells, whereas erythrocyte membranes isolated from wild-type mice exerted osteoinductive effects similar to those of the NO donor diethylenetriamine-NO.

Erythrocyte Membranes From Wild-Type Mice, and to a Lesser Extent Those From eNOS-Deficient Mice, Promote Calcification of Neointimal Lesions in Vivo

To further investigate the cause-effect relationship between eNOS in erythrocytes and vascular lesion calcification in vivo, apoE-deficient mice were fed a Western-type diet for 4 weeks followed by the induction of vascular injury at the common carotid artery. Three weeks later, erythrocyte membranes isolated from either wild-type or eNOS-deficient mice were locally injected into the newly developed neointima to simulate intraplaque hemorrhage and RBC lysis. Representative examples in untreated apoE-deficient mice or mice 10 minutes after the injection of erythrocyte membranes or an equal volume of India ink are shown in Figure IX in the online-only Data Supplement. Analysis of serial cross-sections through vascular lesions 6 weeks after the injection (ie, 9 weeks after injury) revealed that lesion calcification had occurred in 8 of 9 apoE-deficient mice injected with membranes isolated from lysed wild-type erythrocytes (Figure 8A) in comparison with 3 of 7 injected with lysed erythrocyte membranes from eNOS-deficient mice (Figure 8B; it cannot be excluded that injury caused by the injection itself had resulted in extravasation of endogenous RBCs). Of note, vascular calcification was not observed in untreated neointimal lesions, either at the time of injection (Figure IXA and IXB in the online-only Data Supplement) or 6 weeks later (not shown), and also not within spontaneous atherosclerotic plaques at the brachiocephalic artery of those mice (Figure IXD in the online-only Data Supplement). Analysis of atherosclerotic lesions at early (1 and 2 weeks) and late (6 weeks) time points after the injection of RBC membranes revealed the stable presence of the murine erythrocyte membrane marker TER-119 (Figure IXE and IXF in the online-only Data Supplement). Plasma total cholesterol levels were not affected by the local RBC administration (929±55 mg/dL in apoE-deficient mice locally injected

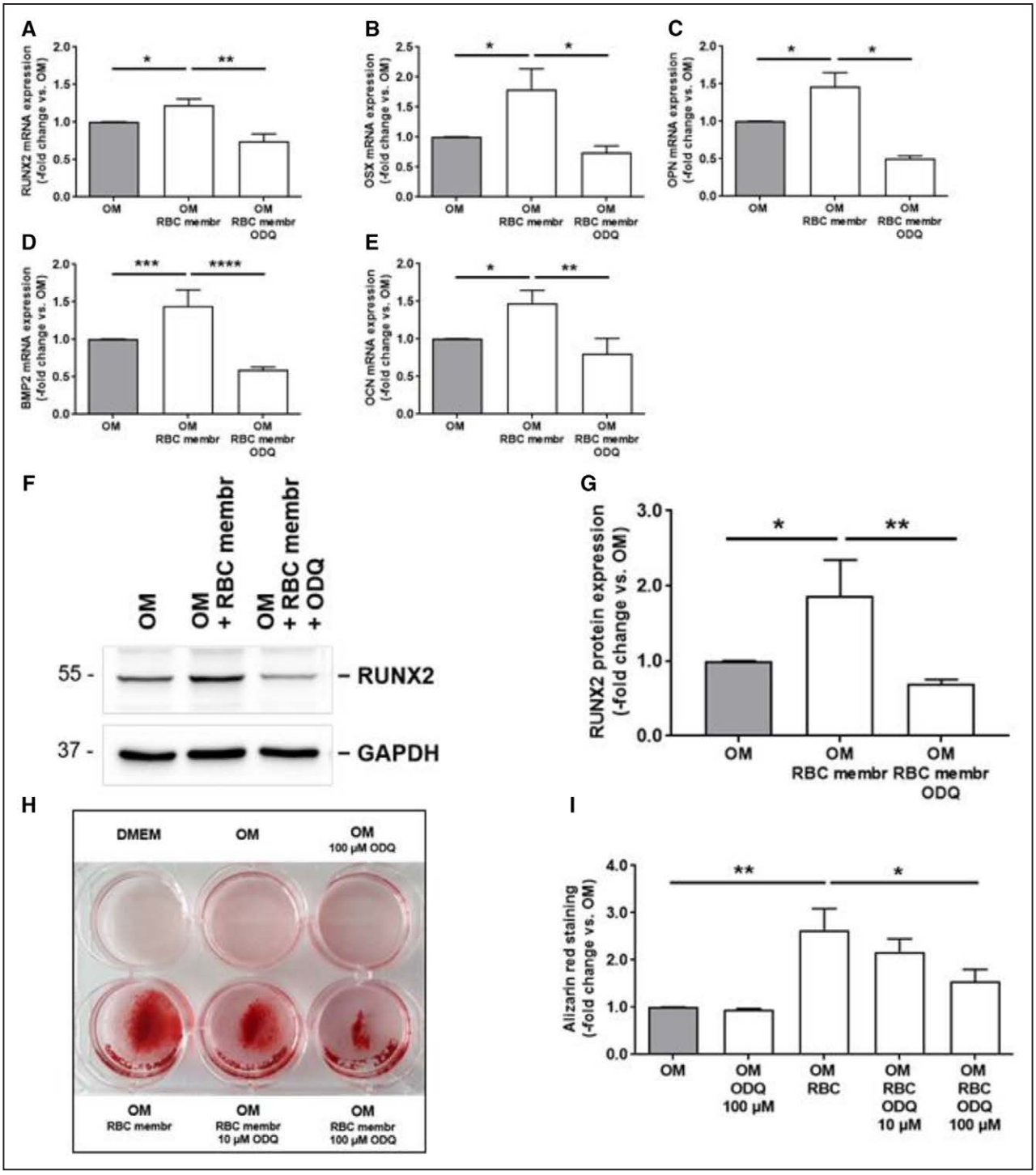

Figure 6. Effect of erythrocyte membranes on osteoblastic marker expression: Importance of NO-induced signaling.
HASMCs were cultivated for 7 days in osteogenic medium (OM) with or without red blood cell (RBC) membranes (membr) or the soluble guanylate cyclase inhibitor ODQ (100 µmol/L). Total RNA was isolated, and the mRNA expression of factors involved in the regulation of osteoblastogenesis, such as RUNX2 (**A**), osterix (OSX; **B**), osteopontin (OPN; **C**), bone morphogenic protein (BMP2; **D**), and osteocalcin (OCN; **E**), were examined using quantitative real-time PCR. The effect of RBC membranes and ODQ on RUNX2 protein levels (**F** and **G**) or calcification (**H** and **I**; Alizarin red staining) was also examined. Representative findings are shown in **F** and **H**; the results of 3 independent experiments are shown in **G** and **I**. **P*<0.05, ***P*<0.01, ****P*<0.001, and *****P*<0.0001. Results shown in **A** to **E**, **G**, and **I** were analyzed using 1-way ANOVA followed by Sidak multiple comparisons test. HASMC indicates human arterial smooth muscle cell; NO, nitric oxide; PCR, polymerase chain reaction; ODQ, 1*H*-[1,2,4]oxadiazolo-[4,3-*a*]quinoxalin-1-one; and RUNX2, runt-related transcription factor-2.

with wild-type lysed erythrocyte membranes; 930±96 mg/dL in those locally injected with RBC membranes from eNOS-deficient mice).

Taken together, our in vitro, ex vivo, and in vivo analyses in murine and human cells and vascular tissue samples suggest that membranes of lysed erythrocytes

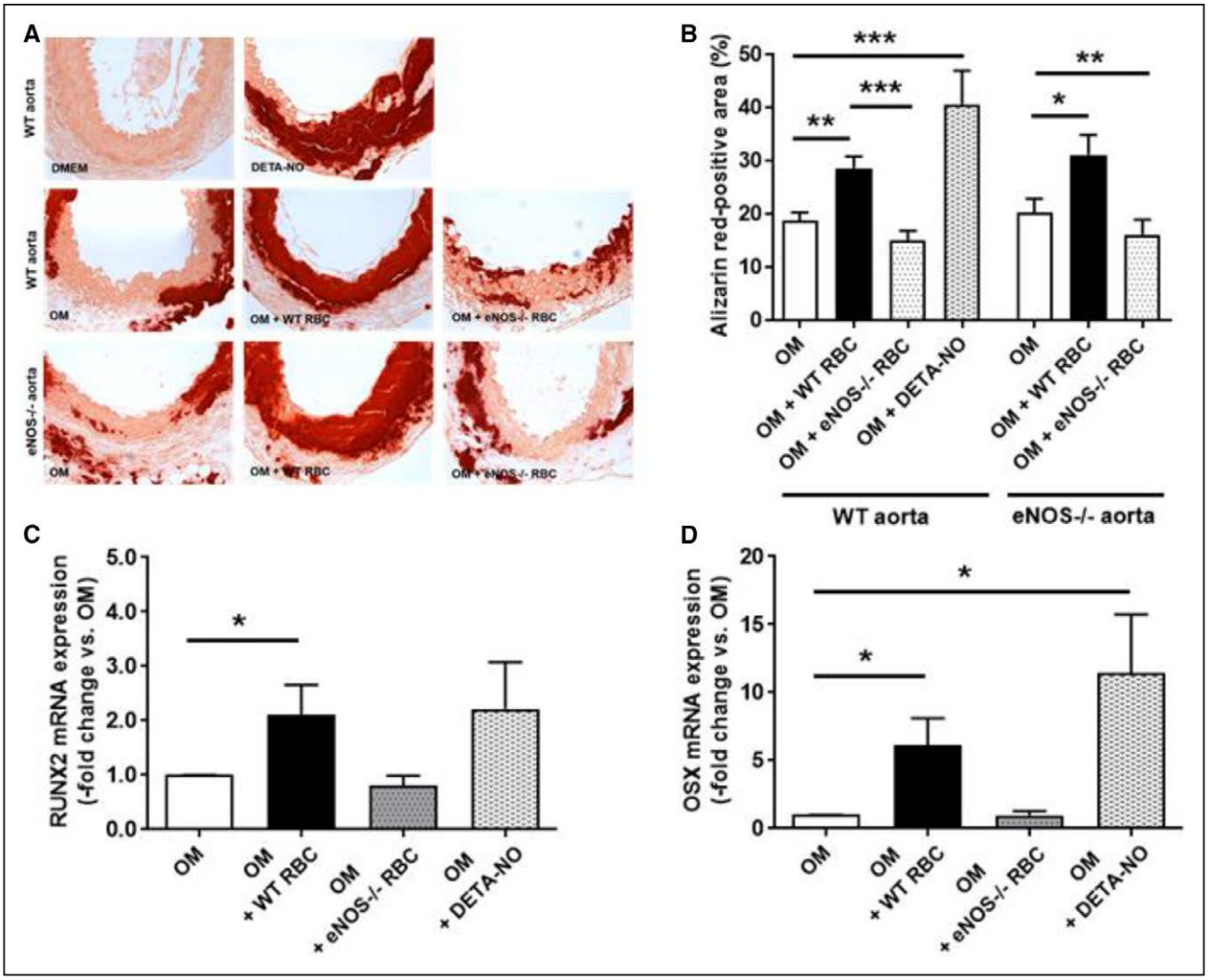

Figure 7. Importance of murine erythrocyte eNOS for smooth muscle cell calcification and osteoblast differentiation ex vivo.
Aortic rings from wild-type (WT) or eNOS-deficient (eNOS$^{-/-}$) mice were incubated in DMEM, osteogenic medium (OM), with or without RBC membranes isolated from lysed erythrocytes of either WT or eNOS$^{-/-}$ mice, followed by staining with Alizarin red (red signal). Representative findings (**A**; ×400 magnification) and the results of the quantitative analysis (**B**) are shown. Murine aortic smooth muscle cells were cultivated for 10 days in DMEM and OM, with or without the addition of lysed RBC membranes from WT or eNOS$^{-/-}$ mice, and the mRNA expression of RUNX2 (**C**) or osterix (OSX; **D**) was examined using real-time PCR. Murine aortic rings or cells incubated with the NO donor DETA-NO were also examined. The summary of 5 experiments is shown. *P<0.05, **P<0.01, and ***P<0.001. Results shown in **B**, **C**, and **D** were analyzed using 1-way ANOVA followed by Sidak multiple comparisons test. DETA indicates diethylenetriamine; eNOS, endothelial nitric oxide synthase; NO, nitric oxide; RBC, red blood cell; and RUNX2, runt-related transcription factor-2.

promote osteogenic differentiation and calcification of vascular smooth muscle cells via local release of NO and NO-dependent signaling.

DISCUSSION

Intraleaflet hemorrhage is observed in almost 80% of specimens from patients with calcific (degenerative) aortic stenosis,[10] and it is also frequent in human and experimental (rabbit) atherosclerotic lesions.[8,9] It is important to note that intraplaque hemorrhage is more extensive in patients with rapid progression of aortic stenosis,[10] and in advanced coronary[8] or carotid[9] lesions, although it has not yet been determined whether the presence of extravasated erythrocytes is the cause or an epiphenomenon of lesion progression. It has been suggested that intramural hemorrhage and erythrocyte cholesterol deposition may promote lipid core expansion and atherosclerosis progression, and accelerate aortic valve degeneration.[9] Based on the findings of the present study, which were obtained (1) in cultured vascular cells, (2) in tissues from genetically modified mice, (3) in an in vivo model of atherosclerosis and neointimal thickening, and (4) by analysis of human arterial wall and aortic valve specimens, we propose a novel pathomechanism, in which lysed RBC membranes directly potentiate osteoblastic differentiation and mineralization of vascular smooth muscle cells and thus calcification of the vessel wall or the affected valve.

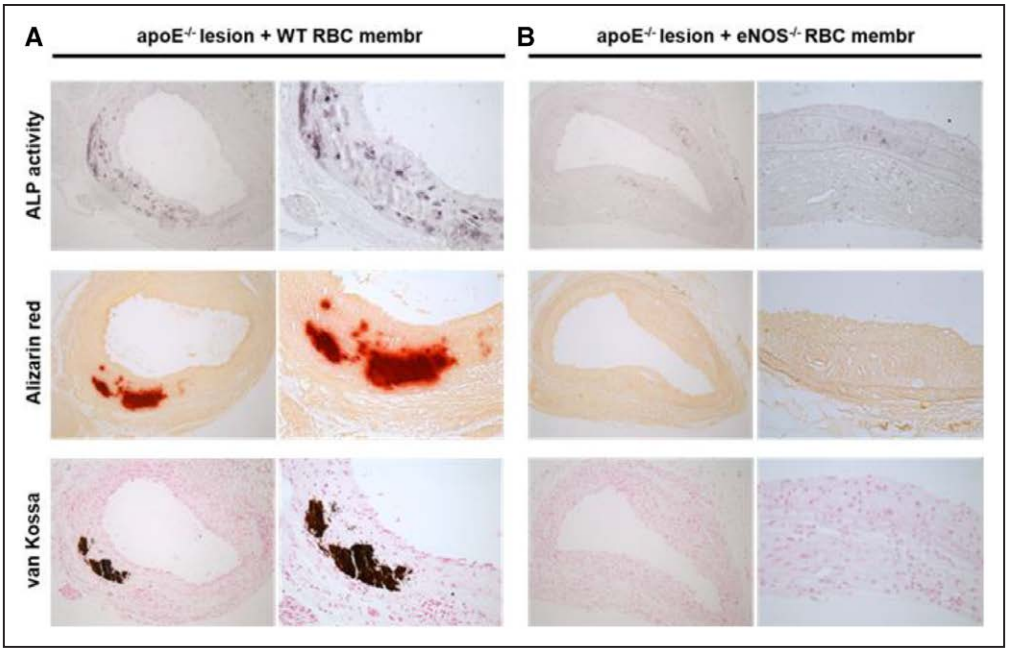

Figure 8. Effect of erythrocyte membranes on atherosclerotic lesion calcification in vivo.
Vascular injury was induced at the common carotid artery of male apolipoprotein E–deficient (apoE$^{-/-}$) mice fed a Western-type diet for 4 weeks. Three weeks later, erythrocyte membranes (5 μL) isolated from either wild-type (WT; **A**) or eNOS-deficient mice (eNOS$^{-/-}$; **B**) were carefully injected into the neointima. Paraffin-embedded serial cross-sections were microscopically examined 6 weeks later for the presence of alkaline phosphatase (ALP) activity or the deposition of calcium (Alizarin red) or phosphate (van Kossa). Examples at ×200 magnification (left column in **A** and **B**) and ×400 magnification (right column in **A** and **B**) are shown. eNOS indicates endothelial nitric oxide synthase; membr, membrane; and RBC, red blood cell.

Effects of Lysed Erythrocyte Membranes on Osteoblastic Differentiation of Smooth Muscle Cells

Vascular calcification is an actively regulated process, in which the activation of specific transcription factors in smooth muscle cells results in the transition to an osteoblast-like phenotype and the incorporation of hydroxyapatite crystals,[4] similar to the steps and signaling pathways occurring during embryonic osteoblastogenesis and differentiation of mesenchymal stem cells. In the present study, we could demonstrate both in human and murine arterial smooth muscle cells that lysed erythrocyte membranes enhance the expression of several typical markers of osteoblastic differentiation. Elevated activity and expression of alkaline phosphatase, osteocalcin, and RUNX2 has been previously reported in human calcified atherosclerotic lesions,[5,24] and our results now suggest that it may have been initiated by intramural hemorrhage. Local hypoxia within vascular lesions promotes the formation of immature and leaky intramural blood vessels from which RBCs can extravasated in the absence of overt vessel rupture.[25] In the highly oxidative environment of atherosclerotic lesions, erythrocytes are rapidly lysed, resulting in the local deposition of their contents, notably cholesterol, iron, and hemoglobin. We have previously shown that erythrocyte cholesterol deposition contributes to human[11,12] and rabbit[13] atherosclerotic lesion progression. Focusing on vascular calcification, we now show that erythrocyte membranes, but not the lipid fraction extracted from them, induce osteoblastic differentiation and calcium deposition. We also could exclude cell death with subsequent passive mineralization as a potential explanation for our findings.

Potential Mechanisms Involved in Erythrocyte-Induced Vascular Calcification

Erythrocytes are anuclear cells whose main function is the transportation of oxygen. Thus, their cytoplasm is rich in iron-containing heme/hemoglobin to which oxygen is reversibly bound and released. Previous analyses revealed that erythrocyte membranes are rich in cholesterol and phospholipids,[12,13] and in structural proteins, as well, which ensure their elasticity and plasticity.[26] It is interesting to note that erythrocytes also express the endothelial isoform of NO synthase (eNOS).[19,20] Studies in mice supported the relevance of erythrocyte-derived NO for cardiovascular (patho-) physiology by demonstrating the contribution of circulating NO pools to blood pressure regulation[27] and left ventricular remodeling following myocardial infarction,[28] among others.

A recent study reported that erythrocytes in whole blood are unable to induce typical NO-mediated signaling, ie, the sGC-cyclic guanosine monophosphate-protein kinase G pathway, in platelets.[29] In intact erythrocytes, NO is bound to oxygenated hemoglobin and thus rapidly inactivated/scavenged,[30] which may

explain the absence of NO-mediated signaling[29] and osteogenic effects of intact erythrocytes in the present study. In our in vitro studies using lysed erythrocyte preparations, separation of the membrane fraction reduced their contamination with heme and hemoglobin, allowing more NO to act on smooth muscle cells. The importance of (oxygenated) hemoglobin as a NO scavenger is further supported by our findings that the reconstitution of erythrocyte membranes with heme, ie, the NO-binding portion of hemoglobin, completely prevented the osteoinductive effects of erythrocyte membranes, similar to the NO scavenger 2-phenyl-4,4,5,5-tetramethylimidazoline-1-oxyl 3-oxide. In addition, the majority of hemoglobin in human vascular lesions was in the form of methemoglobin, in which iron heme is oxidized to the ferric ($^{3+}$) form and does not scavenge NO with the same efficacy as ferrous ($^{2+}$) heme.[31] Macrophages and smooth muscle cells express the hemoglobin scavenger receptor CD163. They may phagocytose hemoglobin released from lysed erythrocytes and thereby remove this potent NO scavenger.[32] Overall, our findings suggest that increased RBC fragility and susceptibility to lysis under mechanical, osmotic, or other local stress may play a role during vascular calcification. Whether and how alterations in factors regulating erythrocyte membrane stability, such as spectrin or essential free fatty acids,[33] affect intraplaque RBC lysis (and ultimately calcification) could not be addressed in the present study.

In our studies, calcification of human and murine arterial smooth muscle cells was also induced by the NO donor diethylenetriamine-NO. Previous studies have shown that NO promotes the differentiation of osteoblasts via phosphorylation of RUNX2 downstream of sGC activation, release of (c)GMP, and activation of protein kinase G.[34,35] We now confirmed and extended those studies by showing that coincubation of HASMCs with lysed erythrocyte membranes increases RUNX2 mRNA and protein levels and mRNA expression of the osteoblast transcription factor osterix and several RUNX2 target genes, and also showing that these effects are sensitive to NO scavenging, inhibition of the NO receptor sGC, or genetic or pharmacological deletion of eNOS. In addition to eNOS, human and murine erythrocytes express arginase-1, which regulates the bioavailability of NO through several mechanisms, including changes in NOS enzyme activity and substrate (ie, L-arginine) competition. A previous study demonstrated that arginase regulates erythrocyte NOS and release of NO.[36] In this regard, we could now show that inhibiting arginase-1 by using L-norvaline promotes vascular calcification and osteoblastic differentiation in an NOS-dependent manner, although we cannot exclude that arginase-1 inhibition may have exerted direct effects on HASMCs.

eNOS Expression in Human Erythrocyte Preparations

In our experiments involving a relatively small number of individuals, lysed erythrocytes isolated from patients with clinically documented coronary artery disease or aortic valve stenosis did not differ from those of healthy controls in the expression levels of eNOS or arginase-1 protein. These preliminary findings suggest that it may be the presence of erythrocytes themselves inside the valve leaflets or vessel wall (as a result of local microhemorrhage), rather than interindividual differences in the RBC expression pattern of osteogenic mediators, that promotes vascular or valvular calcification. However, an earlier study reported that patients with coronary heart disease express reduced levels of eNOS in erythrocytes.[20] The effects of cardiovascular risk factors and atherosclerotic disease on erythrocyte eNOS and arginase-1 expression and their possible impact on vascular calcification need to be explored in future studies involving larger numbers of individuals.

Source of eNOS and Differential Effects of NO on Atherosclerosis

Our results showing a reduced capacity of lysed erythrocyte membranes from eNOS-deficient mice to promote vascular calcification ex vivo and in vivo may appear to contradict the results of earlier studies in mice with global eNOS deficiency crossed into the atherogenic apolipoprotein E knockout background. Because of the prominent role of eNOS-derived NO for vascular function and blood pressure regulation,[37] the enhanced atherosclerotic lesion progression previously reported in apoE-deficient mice lacking eNOS may, at least in part, be an indirect consequence of the endothelial dysfunction and systemic blood pressure elevation present in these mice.[38] Moreover, eNOS is expressed by several cell types present in atherosclerotic lesions, such as smooth muscle cells, immune cells, or platelets, and our analyses confirmed those previous findings (Figure X in the online-only Data Supplement). Thus, the differential effects of cell-specific (rather than global) deletion of eNOS in atherosclerosis warrant further study. Furthermore, calcification and hemorrhage with erythrocyte extravasation typically occur in advanced stages of atherosclerosis, and thus our findings do not contradict previous evidence on the beneficial role of eNOS released from healthy endothelium. The increased aortic valve calcification previously reported in eNOS-deficient mice most likely was associated with the more frequent presence of bicuspid aortic valves, whereas trileaflet eNOS-deficient valves did not develop abnormal calcification.[39] Of note, not only detrimental effects but also

a paradoxical reduction of fatty streak formation and low-density lipoprotein cholesterol oxidation in mice lacking eNOS have been reported.[40] Others observed increased endothelial NO expression reacting with superoxide to form peroxynitrite during advanced atherosclerosis stages[41] that was found to accelerate atherosclerotic lesion formation via increased superoxide generation.[42,43] In this regard, we also examined whether local NO overexpression might induce osteoblast differentiation via increased expression of reactive oxygen species, but found that coincubation with the antioxidants superoxide dismutase and catalase did not block smooth muscle cell mineralization induced by erythrocyte membranes.

The important role of NO in the regulation of osteogenesis has been known for some time (as recently reviewed[44]). For example, osteoblasts were shown to constitutively express eNOS,[45] and stimulation of cultivated osteoblasts or stromal ST2 cells with exogenous NO donors enhanced alkaline phosphatase activity, mineralization, and osteocalcin expression.[46] However, the addition of asymmetric dimethylarginine, an endogenous inhibitor of eNOS, was associated with reduced osteoblast differentiation.[47] Our findings now suggest that NO generated and released from eNOS expressed in erythrocytes may modulate the osteoblastic differentiation of smooth muscle cells and calcification of murine aortas or vascular lesions. Mechanistically, NO could act via activation of sGC, the release of cGMP, and activation of protein kinase G with subsequent phosphorylation of RUNX2 and differentiation into osteoblasts, as previously reported,[33,34,47] and our findings in vitro, ex vivo, and in vivo support a role for this pathway. In addition, NO may act independently of sGC and directly interact with β-catenin,[48] a central signaling molecule during osteoblast differentiation.[49] The signaling pathways in smooth muscle cells involved in their osteoblastic differentiation in response to factors released from lysed erythrocytes clearly need to be investigated in more detail.

CONCLUSIONS

The findings of the present study highlight a novel and potentially important facet of erythrocyte contribution to atherosclerotic and valvular lesion progression by proposing a direct and active role of intramural or intraleaflet microhemorrhage in valvular and vascular lesion calcification. Analysis of potential mediators of osteogenic activity revealed a role for erythrocyte-derived NO, and vascular calcification could be modulated by regulating eNOS activity and NO release from erythrocytes or signaling via the NO receptor. These findings may have important implications for better understanding and possibly preventing advanced atherosclerosis and calcific valvular disease.

ARTICLE INFORMATION

Received August 12, 2018; accepted January 10, 2019.

The online-only Data Supplement is available with this article at https://www.ahajournals.org/doi/suppl/10.1161/CIRCULATIONAHA.118.037166.

Correspondence

Katrin Schäfer, MD, FAHA, FESC, Center for Cardiology, Cardiology I, University Medical Center of the Johannes Gutenberg University Mainz, Langenbeckstraße 1, D-55131 Mainz, Germany. Email katrin.schaefer@unimedizin-mainz.de

Affiliations

Department of Cardiology (D.N.T., G.C., M.P., D.K., P.S., I.D., P.K., S.V.K.), Cardiothoracic Surgery Department (D.M., F.K.), Department of Pathology (A.G.), Department of Vascular Surgery (G.S.G., C.A.), Democritus University of Thrace, Alexandroupolis, Greece. Center for Cardiology, Cardiology I (R.G., A.H., E.B., I.D., T.M., K.S.), Center for Thrombosis and Hemostasis (S.V.K.), University Medical Center of the Johannes Gutenberg University Mainz, Germany.

Acknowledgments

The authors thank M. Janocha, A. Kern, and K. Rost for expert technical assistance. The authors are grateful to Drs Kelm and Cortese-Krott (University Hospital Düsseldorf, Germany, Department of Cardiology, Angiology and Pulmonology) for helpful discussions regarding erythrocyte endothelial nitric oxide synthase and to Drs Li and Xia (University Medical Center Mainz, Germany, Institute of Pharmacology) and Professor Danckwardt for providing eNOS- and apolipoprotein E–deficient mice, respectively. Results shown in this study are part of the medical thesis of E. Böhm.

Sources of Funding

This work was supported by the German Research Foundation (Deutsche Forschungsgemeinschaft; Scha 808/9-1 to Dr Schäfer), the Bundesministerium für Bildung und Forschung (BMBF 01E01003 and BMBF 01E0503 to Dr Konstantinides), a research grant by the European Society of Cardiology to Dr Kareli, and by Greek and European Union funds from the 'Operational Programme Education and Lifelong Learning (NSRF 2007–2013) MIS 379527' to Drs Tziakas, Konstantinides, and Schäfer.

Disclosures

None.

REFERENCES

1. Allison MA, Criqui MH, Wright CM. Patterns and risk factors for systemic calcified atherosclerosis. *Arterioscler Thromb Vasc Biol*. 2004;24:331–336. doi: 10.1161/01.ATV.0000110786.02097.0c
2. Maldonado N, Kelly-Arnold A, Vengrenyuk Y, Laudier D, Fallon JT, Virmani R, Cardoso L, Weinbaum S. A mechanistic analysis of the role of microcalcifications in atherosclerotic plaque stability: potential implications for plaque rupture. *Am J Physiol Heart Circ Physiol*. 2012;303:H619–H628. doi: 10.1152/ajpheart.00036.2012
3. Boström KI, Rajamannan NM, Towler DA. The regulation of valvular and vascular sclerosis by osteogenic morphogens. *Circ Res*. 2011;109:564–577. doi: 10.1161/CIRCRESAHA.110.234278
4. Rajamannan NM, Subramaniam M, Rickard D, Stock SR, Donovan J, Springett M, Orszulak T, Fullerton DA, Tajik AJ, Bonow RO, Spelsberg T. Human aortic valve calcification is associated with an osteoblast phenotype. *Circulation*. 2003;107:2181–2184. doi: 10.1161/01.CIR.0000070591.21548.69
5. Tyson KL, Reynolds JL, McNair R, Zhang Q, Weissberg PL, Shanahan CM. Osteo/chondrocytic transcription factors and their target genes exhibit distinct patterns of expression in human arterial calcification. *Arterioscler Thromb Vasc Biol*. 2003;23:489–494. doi: 10.1161/01.ATV.0000059406.92165.31
6. Tanaka K, Sata M, Fukuda D, Suematsu Y, Motomura N, Takamoto S, Hirata Y, Nagai R. Age-associated aortic stenosis in apolipoprotein E-deficient mice. *J Am Coll Cardiol*. 2005;46:134–141. doi: 10.1016/j.jacc.2005.03.058
7. Virmani R, Roberts WC. Extravasated erythrocytes, iron, and fibrin in atherosclerotic plaques of coronary arteries in fatal coronary heart disease

and their relation to luminal thrombus: frequency and significance in 57 necropsy patients and in 2958 five mm segments of 224 major epicardial coronary arteries. *Am Heart J*. 1983;105:788–797.
8. Kolodgie FD, Gold HK, Burke AP, Fowler DR, Kruth HS, Weber DK, Farb A, Guerrero LJ, Hayase M, Kutys R, Narula J, Finn AV, Virmani R. Intraplaque hemorrhage and progression of coronary atheroma. *N Engl J Med*. 2003;349:2316–2325. doi: 10.1056/NEJMoa035655
9. Takaya N, Yuan C, Chu B, Saam T, Polissar NL, Jarvik GP, Isaac C, McDonough J, Natiello C, Small R, Ferguson MS, Hatsukami TS. Presence of intraplaque hemorrhage stimulates progression of carotid atherosclerotic plaques: a high-resolution magnetic resonance imaging study. *Circulation*. 2005;111:2768–2775. doi: 10.1161/CIRCULATIONAHA.104.504167
10. Akahori H, Tsujino T, Naito Y, Matsumoto M, Lee-Kawabata M, Ohyanagi M, Mitsuno M, Miyamoto Y, Daimon T, Hao H, Hirota S, Masuyama T. Intraleaflet haemorrhage is associated with rapid progression of degenerative aortic valve stenosis. *Eur Heart J*. 2011;32:888–896. doi: 10.1093/eurheartj/ehq479
11. Tziakas DN, Kaski JC, Chalikias GK, Romero C, Fredericks S, Tentes IK, Kortsaris AX, Hatseras DI, Holt DW. Total cholesterol content of erythrocyte membranes is increased in patients with acute coronary syndrome: a new marker of clinical instability? *J Am Coll Cardiol*. 2007;49:2081–2089. doi: 10.1016/j.jacc.2006.08.069
12. Tziakas DN, Chalikias GK, Stakos D, Tentes IK, Chatzikyriakou SV, Mitrousi K, Kortsaris AX, Boudoulas H, Kaski JC. Cholesterol composition of erythrocyte membranes and its association with clinical presentation of coronary artery disease. *Coron Artery Dis*. 2008;19:583–590. doi: 10.1097/MCA.0b013e328313819b
13. Tziakas D, Chalikias G, Kapelouzou A, Tentes I, Schäfer K, Karayannakos P, Kostakis A, Boudoulas H, Konstantinides S. Erythrocyte membrane cholesterol and lipid core growth in a rabbit model of atherosclerosis: modulatory effects of rosuvastatin. *Int J Cardiol*. 2013;170:173–181. doi: 10.1016/j.ijcard.2013.10.070
14. Paul A, Calleja L, Vilella E, Martínez R, Osada J, Joven J. Reduced progression of atherosclerosis in apolipoprotein E-deficient mice with phenylhydrazine-induced anemia. *Atherosclerosis*. 1999;147:61–68.
15. Tziakas DN, Chalikias GK, Tentes IK, Stakos D, Chatzikyriakou SV, Mitrousi K, Kortsaris AX, Kaski JC, Boudoulas H. Interleukin-8 is increased in the membrane of circulating erythrocytes in patients with acute coronary syndrome. *Eur Heart J*. 2008;29:2713–2722. doi: 10.1093/eurheartj/ehn382
16. Folch J, Lees M, Sloane Stanley GH. A simple method for the isolation and purification of total lipides from animal tissues. *J Biol Chem*. 1957;226:497–509.
17. Egyed A. A simple method for heme isolation. *Experientia*. 1972;28:1396–1397.
18. Gregory CA, Gunn WG, Peister A, Prockop DJ. An Alizarin red-based assay of mineralization by adherent cells in culture: comparison with cetylpyridinium chloride extraction. *Anal Biochem*. 2004;329:77–84. doi: 10.1016/j.ab.2004.02.002
19. Kleinbongard P, Schulz R, Rassaf T, Lauer T, Dejam A, Jax T, Kumara I, Gharini P, Kabanova S, Ozüyaman B, Schnürch HG, Gödecke A, Weber AA, Robenek M, Robenek H, Bloch W, Rösen P, Kelm M. Red blood cells express a functional endothelial nitric oxide synthase. *Blood*. 2006;107:2943–2951. doi: 10.1182/blood-2005-10-3992
20. Cortese-Krott MM, Rodriguez-Mateos A, Sansone R, Kuhnle GG, Thasian-Sivarajah S, Krenz T, Horn P, Krisp C, Wolters D, Heiß C, Kröncke KD, Hogg N, Feelisch M, Kelm M. Human red blood cells at work: identification and visualization of erythrocytic eNOS activity in health and disease. *Blood*. 2012;120:4229–4237. doi: 10.1182/blood-2012-07-442277
21. Harris MB, Blackstone MA, Ju H, Venema VJ, Venema RC. Heat-induced increases in endothelial NO synthase expression and activity and endothelial NO release. *Am J Physiol Heart Circ Physiol*. 2003;285:H333–H340. doi: 10.1152/ajpheart.00726.2002
22. Chen CA, Wang TY, Varadharaj S, Reyes LA, Hemann C, Talukder MA, Chen YR, Druhan LJ, Zweier JL. S-glutathionylation uncouples eNOS and regulates its cellular and vascular function. *Nature*. 2010;468:1115–1118. doi: 10.1038/nature09599
23. Ducy P, Zhang R, Geoffroy V, Ridall AL, Karsenty G. Osf2/Cbfa1: a transcriptional activator of osteoblast differentiation. *Cell*. 1997;89:747–754.
24. Sluimer JC, Kolodgie FD, Bijnens AP, Maxfield K, Pacheco E, Kutys B, Duimel H, Frederik PM, van Hinsbergh VW, Virmani R, Daemen MJ. Differential expression of bone matrix regulatory proteins in human atherosclerotic plaques. *Arterioscler Thromb Vasc Biol*. 2001;21:1998–2003.
25. Sluimer JC, Kolodgie FD, Bijnens AP, Maxfield K, Pacheco E, Kutys B, Duimel H, Frederik PM, van Hinsbergh VW, Virmani R, Daemen MJ. Thin-walled microvessels in human coronary atherosclerotic plaques show incomplete endothelial junctions relevance of compromised structural integrity for intraplaque microvascular leakage. *J Am Coll Cardiol*. 2009;53:1517–1527. doi: 10.1016/j.jacc.2008.12.056
26. Kakhniashvili DG, Bulla LA Jr, Goodman SR. The human erythrocyte proteome: analysis by ion trap mass spectrometry. *Mol Cell Proteomics*. 2004;3:501–509. doi: 10.1074/mcp.M300132-MCP200
27. Wood KC, Cortese-Krott MM, Kovacic JC, Noguchi A, Liu VB, Wang X, Raghavachari N, Boehm M, Kato GJ, Kelm M, Gladwin MT. Circulating blood endothelial nitric oxide synthase contributes to the regulation of systemic blood pressure and nitrite homeostasis. *Arterioscler Thromb Vasc Biol*. 2013;33:1861–1871. doi: 10.1161/ATVBAHA.112.301068
28. Gorressen S, Stern M, van de Sandt AM, Cortese-Krott MM, Ohlig J, Rassaf T, Gödecke A, Fischer JW, Heusch G, Merx MW, Kelm M. Circulating NOS3 modulates left ventricular remodeling following reperfused myocardial infarction. *PLoS One*. 2015;10:e0120961. doi: 10.1371/journal.pone.0120961
29. Gambaryan S, Subramanian H, Kehrer L, Mindukshev I, Sudnitsyna J, Reiss C, Rukoyatkina N, Friebe A, Sharina I, Martin E, Walter U. Erythrocytes do not activate purified and platelet soluble guanylate cyclases even in conditions favourable for NO synthesis. *Cell Commun Signal*. 2016;14:16. doi: 10.1186/s12964-016-0139-9
30. Joshi MS, Ferguson TB Jr, Han TH, Hyduke DR, Liao JC, Rassaf T, Bryan N, Feelisch M, Lancaster JR Jr. Nitric oxide is consumed, rather than conserved, by reaction with oxyhemoglobin under physiological conditions. *Proc Natl Acad Sci USA*. 2002;99:10341–10346. doi: 10.1073/pnas.152149699
31. Helms C, Kim-Shapiro DB. Hemoglobin-mediated nitric oxide signaling. *Free Radic Biol Med*. 2013;61:464–472. doi: 10.1016/j.freeradbiomed.2013.04.028
32. Weidenbach H, Massmann J. Erythrocytophagocytosis by arterial smooth muscle cells in experimental atherosclerosis. *Exp Pathol (Jena)*. 1978;15:111–115.
33. Zavodnik IB, Lapshina EA, Palecz D, Bryszewska M. The effects of palmitate on human erythrocyte membrane potential and osmotic stability. *Scand J Clin Lab Invest*. 1996;56:401–407.
34. Marathe N, Rangaswami H, Zhuang S, Boss GR, Pilz RB. Pro-survival effects of 17β-estradiol on osteocytes are mediated by nitric oxide/cGMP via differential actions of cGMP-dependent protein kinases I and II. *J Biol Chem*. 2012;287:978–988. doi: 10.1074/jbc.M111.294959
35. Pan W, Quarles LD, Song LH, Yu YH, Jiao C, Tang HB, Jiang CH, Deng HW, Li YJ, Zhou HH, Xiao ZS. Genistein stimulates the osteoblastic differentiation via NO/cGMP in bone marrow culture. *J Cell Biochem*. 2005;94:307–316. doi: 10.1002/jcb.20308
36. Yang J, Gonon AT, Sjöquist PO, Lundberg JO, Pernow J. Arginase regulates red blood cell nitric oxide synthase and export of cardioprotective nitric oxide bioactivity. *Proc Natl Acad Sci USA*. 2013;110:15049–15054. doi: 10.1073/pnas.1307058110
37. Huang PL, Huang Z, Mashimo H, Bloch KD, Moskowitz MA, Bevan JA, Fishman MC. Hypertension in mice lacking the gene for endothelial nitric oxide synthase. *Nature*. 1995;377:239–242. doi: 10.1038/377239a0
38. Kuhlencordt PJ, Gyurko R, Han F, Scherrer-Crosbie M, Aretz TH, Hajjar R, Picard MH, Huang PL. Accelerated atherosclerosis, aortic aneurysm formation, and ischemic heart disease in apolipoprotein E/endothelial nitric oxide synthase double-knockout mice. *Circulation*. 2001;104:448–454.
39. El Accaoui RN, Gould ST, Hajj GP, Chu Y, Davis MK, Kraft DC, Lund DD, Brooks RM, Doshi H, Zimmerman KA, Kutschke W, Anseth KS, Heistad DD, Weiss RM. Aortic valve sclerosis in mice deficient in endothelial nitric oxide synthase. *Am J Physiol Heart Circ Physiol*. 2014;306:H1302–H1313. doi: 10.1152/ajpheart.00392.2013
40. Shi W, Wang X, Shih DM, Laubach VE, Navab M, Lusis AJ. Paradoxical reduction of fatty streak formation in mice lacking endothelial nitric oxide synthase. *Circulation*. 2002;105:2078–2082.
41. Bouloumié A, Bauersachs J, Linz W, Schölkens BA, Wiemer G, Fleming I, Busse R. Endothelial dysfunction coincides with an enhanced nitric oxide synthase expression and superoxide anion production. *Hypertension*. 1997;30:934–941.
42. Ozaki M, Kawashima S, Yamashita T, Hirase T, Namiki M, Inoue N, Hirata K, Yasui H, Sakurai H, Yoshida Y, Masada M, Yokoyama M. Overexpression of endothelial nitric oxide synthase accelerates atherosclerotic lesion formation in apoE-deficient mice. *J Clin Invest*. 2002;110:331–340. doi: 10.1172/JCI15215
43. Takaya T, Hirata K, Yamashita T, Shinohara M, Sasaki N, Inoue N, Yada T, Goto M, Fukatsu A, Hayashi T, Alp NJ, Channon KM, Yokoyama M, Kawashima S. A specific role for eNOS-derived reactive oxygen species in

atherosclerosis progression. *Arterioscler Thromb Vasc Biol*. 2007;27:1632–1637. doi: 10.1161/ATVBAHA.107.142182
44. Kalyanaraman H, Schall N, Pilz RB. Nitric oxide and cyclic GMP functions in bone. *Nitric Oxide*. 2018;76:62–70. doi: 10.1016/j.niox.2018.03.007
45. Helfrich MH, Evans DE, Grabowski PS, Pollock JS, Ohshima H, Ralston SH. Expression of nitric oxide synthase isoforms in bone and bone cell cultures. *J Bone Miner Res*. 1997;12:1108–1115. doi: 10.1359/jbmr.1997.12.7.1108
46. Ehnes DD, Geransar RM, Rancourt DE, Zur Nieden NI. Exogenous nitric oxide enhances calcification in embryonic stem cell-derived osteogenic cultures. *Differentiation*. 2015;89:97–103. doi: 10.1016/j.diff.2015.02.001
47. Xiao ZS, Quarles LD, Chen QQ, Yu YH, Qu XP, Jiang CH, Deng HW, Li YJ, Zhou HH. Effect of asymmetric dimethylarginine on osteoblastic differentiation. *Kidney Int*. 2001;60:1699–1704. doi: 10.1046/j.1523-1755.2001.00011.x
48. Warboys CM, Chen N, Zhang Q, Shaifta Y, Vanderslott G, Passacquale G, Hu Y, Xu Q, Ward JP, Ferro A. Bidirectional cross-regulation between the endothelial nitric oxide synthase and β-catenin signalling pathways. *Cardiovasc Res*. 2014;104:116–126. doi: 10.1093/cvr/cvu173
49. Ding H, Keller KC, Martinez IK, Geransar RM, zur Nieden KO, Nishikawa SG, Rancourt DE, zur Nieden NI. NO-β-catenin crosstalk modulates primitive streak formation prior to embryonic stem cell osteogenic differentiation. *J Cell Sci*. 2012;125(pt 22):5564–5577. doi: 10.1242/jcs.081703